doi:10.1093/plphys/kiab146 PLANT PHYSIOLOGY 2021: 186: 853–864

Plant Physiology®

Breakthrough Tech

A tobacco ringspot virus-based vector system for gene and microRNA function studies in cucurbits

Le Fang,[1] Xin-Yu Wei,[1] Ling-Zhi Liu,[1] Ling-Xi Zhou,[1] Yan-Ping Tian,[1] Chao Geng [1,*] and Xiang-Dong Li [1,†]

1 Shandong Provincial Key Laboratory of Agricultural Microbiology, Department of Plant Pathology, College of Plant Protection, Shandong Agricultural University, Tai'an, Shandong 271018, China

*Author for communication: chaogeng@sdau.edu.cn
†Senior author.

C.G. and X.-D.L. conceived the research plan and designed the experiments. L.F. and X.-Y.W performed the experiments and prepare the Figures and Tables. C.G., X.-D.L., and L.F. co-wrote and edited the article. All authors analyzed the results.
The authors responsible for distribution of materials integral to the findings presented in this article in accordance with the policy described in the Instructions for Authors (https://academic.oup.com/plphys/pages/general-instructions) are: Chao Geng (chaogeng@sdau.edu.cn) and Xiang-Dong Li (xdongli@sdau.edu.cn).

Abstract

Cucurbits are economically important crops worldwide. The genomic data of many cucurbits are now available. However, functional analyses of cucurbit genes and noncoding RNAs have been impeded because genetic transformation is difficult for many cucurbitaceous plants. Here, we developed a set of tobacco ringspot virus (TRSV)-based vectors for gene and microRNA (miRNA) function studies in cucurbits. A TRSV-based expression vector could simultaneously express GREEN FLUORESCENT PROTEIN (GFP) and heterologous viral suppressors of RNA silencing in TRSV-infected plants, while a TRSV-based gene silencing vector could knock down endogenous genes exemplified by *PHYTOENE DESATURASE* (*PDS*) in *Cucumis melo*, *Citrullus lanatus*, *Cucumis sativus*, and *Nicotiana benthamiana* plants. We also developed a TRSV-based miRNA silencing vector to dissect the functions of endogenous miRNAs. Four representative miRNAs, namely, miR159, miR166, miR172, and miR319, from different cucurbits were inserted into the TRSV vector using a short tandem target mimic strategy and induced characteristic phenotypes in TRSV-miRNA-infected plants. This TRSV-based vector system will facilitate functional genomic studies in cucurbits.

Introduction

Cucurbits, including cucumber (*Cucumis sativus*), melon (*Cucumis melo*), watermelon (*Citrullus lanatus*), and zucchini (*Cucurbita pepo*), are economically important vegetables globally. Although the genomic sequencing of many cucurbits has been completed (Huang et al., 2009; Garcia-Mas et al., 2012; Guo et al., 2013; Shin et al., 2019; Wu et al., 2019; Wu et al., 2020), the functions of most miRNA or noncoding RNA have not yet been characterized. Some cucurbitaceous plants are highly recalcitrant to genetic transformation, while in others it takes a long time to obtain transgenic plants, which impedes functional genomic studies in cucurbits.

A virus-based gene delivery system is an attractive, quick, and promising approach for the transient gain- and loss-of-function studies in plants recalcitrant to genetic transformation (Zhang and Ghabrial, 2006; Seo et al., 2016; Ding et al., 2018). For the overexpression of a gene in vivo, plant virus-based vectors can elevate the amount of protein in a short time (Gleba et al., 2007; Baltes et al., 2014). For the knockdown of plant genes, plant virus-induced gene silencing has been widely employed as a fast and convenient tool in plant biology studies (Liu et al., 2002; Robertson, 2004; Bachan

Received January 09, 2021. Accepted March 11, 2021. Advance access publication March 25, 2021

and Dinesh-Kumar, 2012; Senthil-Kumar and Mysore, 2014). Recently, some plant RNA or DNA viruses, including barley stripe mosaic virus, Chinese wheat mosaic virus, cotton leaf crumple virus, cucumber mosaic virus (CMV), potato virus X (PVX), and tobacco rattle virus, have been engineered into virus-based miRNA silencing (VbMS) vectors to inhibit the miRNA function in maize (*Zea mays*), wheat (*Triticum aestivum*), *cotton* (*Gossypium hirsutum*), Arabidopsis (*Arabidopsis thaliana*), potato (*Solanum tuberosum*), and *Nicotiana benthamiana* (Du et al., 2014; Gu et al., 2014; Sha et al., 2014; Jiao et al., 2015; Liao et al., 2015; Jian et al., 2017; Yang et al., 2018; Zhao et al., 2020). However, to the best of our knowledge, there has been no virus-based miRNA silencing tool developed for cucurbits up to now.

Two reciprocal reverse genetic strategies have been used to dissect the function of a specific miRNA. For gain-of-function studies, the miRNA activity can be enhanced through transgenically overexpressing miRNA (Sainsbury et al., 2010; Zhang et al., 2013; Yang et al., 2015). For loss-of-function studies, miRNA activity can be blocked by expressing a miRNA-resistant target that contains uncleavable mutations in the miRNA-binding sequence (Javier et al., 2003; Franco-Zorrilla et al., 2007). Some alternative approaches, including miRNA target mimicry (Franco-Zorrilla et al., 2007), short tandem target mimic (STTM; Yan et al., 2012), transcriptional gene silencing of miRNA gene promoters (Vaistij et al., 2010), and artificial miRNA-directed silencing of miRNA precursors (Eamens et al., 2011), have also been applied in the function investigation of miRNA. The above approaches all require time-consuming and expensive transformation. Furthermore, transgenic approaches are not applicable to all cucurbit species. Therefore, it is necessary to develop a fast and efficient approach to investigate the function of cucurbit miRNAs.

Tobacco ringspot virus (TRSV; genus *Nepovirus*, family *Secoviridae*) can infect plants including cucurbits, soybean, blueberry, and *N. benthamiana* (Zellner et al., 2011; Abdalla et al., 2012; Shakiba et al., 2012; Zhao et al., 2015). The genome of TRSV consists of two single-stranded RNAs. RNA1 contains an open reading frame encoding a polyprotein precursor, which is then cleaved into five mature proteins designated as32K, helicase, genome-linked protein, protease, and RNA-dependent RNA polymerase. The RNA2 encodes a polyprotein that can be cleaved into three mature proteins, namely, 2a, movement protein (MP), and coat protein (CP).

In this study, we first engineered TRSV into a gene expression vector, which can simultaneously express two proteins in virus-infected plants, and a gene-silencing vector to knock down the expression of the *PDS* gene in four kinds of plants. Then, we engineered TRSV into a VbMS vector to investigate the biological roles of four representative miRNAs in different cucurbitaceous crops.

Results

Engineering of TRSV as a gene expression vector

To determine whether TRSV can be used to express foreign genes, we cloned its genomic RNA1 and RNA2 into the binary vector pCB301 to generate plasmids pTRSV1 and pTRSV2, respectively. Then, the sequences coding GREEN FLUORESCENT PROTEIN (GFP) and thosea asigna virus 2A (T2A) catalytic peptide were inserted after the coding sequence for the MP/CP cleavage site in pTRSV2, producing pTRSV2-GFP (Figure 1A). The *Agrobacterium tumefaciens* cells harboring pTRSV1 and pTRSV2-GFP were infiltrated into leaves of *Luffa aegyptiaca* and *N. benthamiana* plants. Green fluorescence appeared in the noninoculated upper (i.e. systemic) leaves at 7 d post agroinfiltration (dpai), but became weak and disappeared in 10–12 d along with viral symptom recovery (Figure 1B). To overcome this disadvantage, we tested whether the co-expression of heterologous viral suppressors of RNA silencing (VSRs) could increase the foreign gene's expression level. The coding sequences of three VSRs, namely, the flock house virus (FHV) B2, tomato bushy stunt virus (TBSV) P19, and CMV 2b, were individually inserted into plasmid pTRSV2-GFP through *T2A* and porcine teschovirus-1 *2A* (*P2A*) in tandem, and the resulting plasmids were designated as pTRSV2-GFP-B2, pTRSV2-GFP-P19, and pTRSV2-GFP-2b, respectively (Figure 1A). Upon co-agroinfiltration of each construct with pTRSV1 into *L. aegyptiaca* and *N. benthamiana* plants, much brighter green fluorescence appeared at 12 dpai (Figure 1B), indicating that the expression of heterologous VSRs could significantly increase GFP expression. Western blot analysis of total proteins extracted from virus-infected *L. aegyptiaca* and *N. benthamiana* leaves using a GFP antibody showed that two bands corresponding to GFP-2A and GFP, respectively, were detected in TRSV-GFP-VSRs-infected plants, less protein was detected in TRSV-GFP-infected plants, and no protein was detected in the mock-inoculated plants (Figure 1, C and D). These results showed that the newly modified TRSV-based vector can significantly increase the expression levels of foreign proteins.

Development of TRSV as a virus-induced gene silencing vector

Virus-induced gene silencing (VIGS) is widely used to investigate the function of genes (Liu et al., 2002; Senthil-Kumar and Mysore, 2014; Choi et al., 2019). Because TRSV only caused mild symptoms, we hypothesized that TRSV could be modified as a VIGS vector. To test this point, we inserted a 300-bp fragment of *C. melo PHYTOENE DESATURASE* (*PDS*) into pTRSV2 to generate pTRSV2-CmPDS (Figure 2A). The plasmids pTRSV2-CmPDS and pTRSV1 were first agroinfiltrated into *N. benthamiana* plants. After 7 dpai, the extracts of systemically infected leaves were used as inoculum for *C. melo*, *C. lanatus*, and *C. sativus* plants. Nearly all of the systematically infected leaves became completely white at 18 dpi (Figure 2B). In contrast, the control plants inoculated with TRSV showed no photo-bleaching phenotype. The results of three independent experiments showed that the silencing efficiency could reach 75.0%–100.0% in *C. melo* and *C. lanatus*, and 33.3%–41.7% in *C. sativus* (Supplemental Table S1). The VIGS experiments were also performed in *N. benthamiana* plants. The systemic leaves

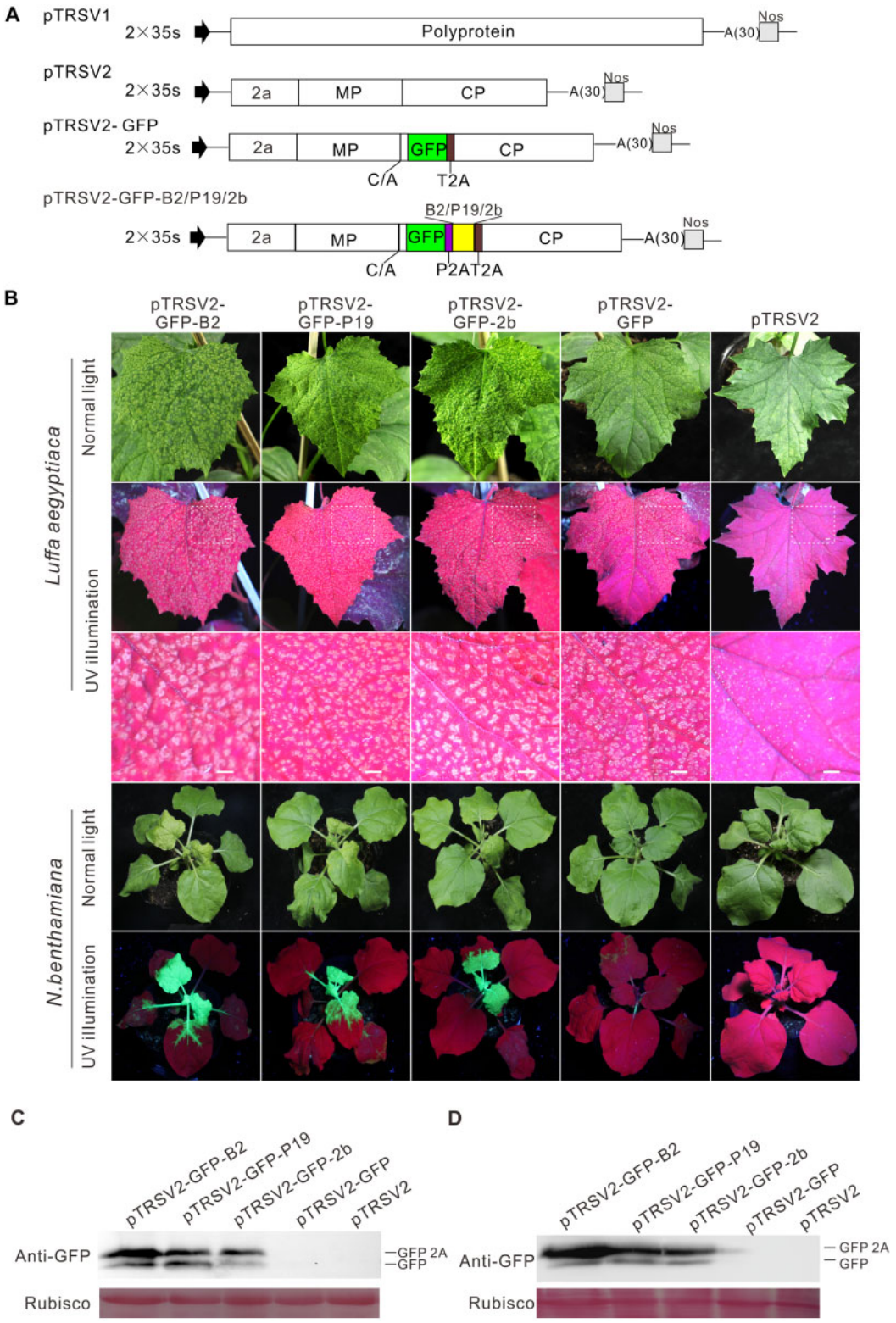

Figure 1 TRSV-based gene expression in *L. aegyptiaca* and *N. benthamiana* plants. A, Schemes of TRSV infectious clone and derivatives. The full-length sequences of RNA1 and RNA2 were inserted between a duplicated cauliflower mosaic virus 35S promoter (2x35S) and the NOS terminator (Nos). To construct pTRSV2-GFP, the *GFP* gene and the sequence encoding thosea asigna virus 2A (T2A) were inserted after the coding sequence for the MOVEMENT PROTEIN/COAT PROTEIN (MP/CP) cleavage site (C/A). Heterologous VSRs and GFP were simultaneously expressed and separated by porcine teschovirus-1 2A (P2A) and T2A in TRSV-based dual genes expression vectors. The release of GFP relied on 2A mediated self-cleavage and polyprotein cleavage. B, Effects of heterologous VSRs on GFP expression using TRSV-based expression vectors in plants at 12 dpai. Symptoms and fluorescence signals of *L. aegyptiaca* and *N. benthamiana* infected with TRSV-GFP-B2, -GFP-P19, -GFP-2b, -GFP, and the control pTRSV2. Scale bars= 1 cm in the second row. The third row shows a magnification of dotted rectangle regions in the second row. C and D, Effects of heterologous VSRs on GFP expression in *L. aegyptiaca* and *N. benthamiana* leaves as determined with Western blotting

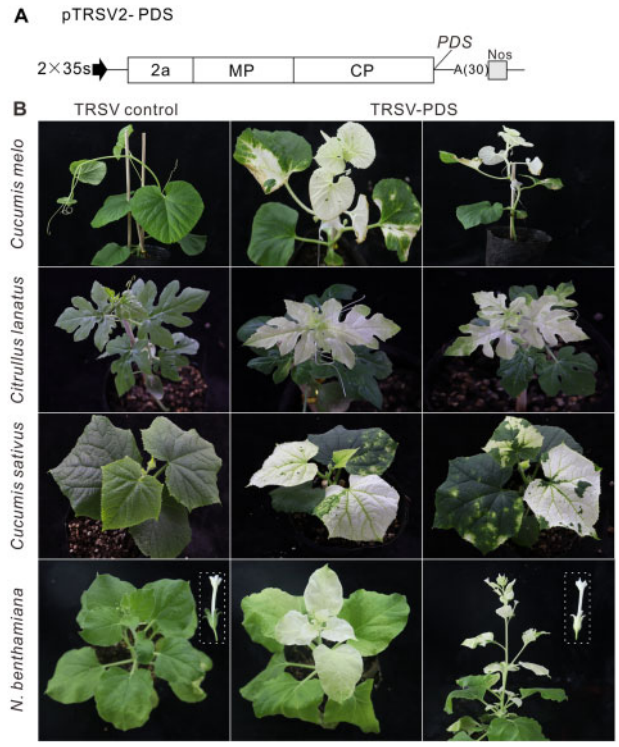

Figure 2 Engineering TRSV as a VIGS vector. A, Schematic representation of pTRSV2. The *Sna* BI restriction enzyme site was inserted into pTRSV2 downstream of the *CP* stop codon. The PCR products of the respective *PDS* genes from cucurbits and *N. benthamiana* genome were digested with *Sna* BI and cloned into pTRSV2. B, Phenotypes of *PDS*-silenced *C. melo*, *C. lanatus*, *C. sativus*, and *N. benthamiana* plants at 18 dpai. The boxes indicate the flowers of TRSV control and TRSV-PDS-infected *N. benthamiana* plants. The experiment was independently repeated three times

and even the flowers of TRSV2-NbPDS-infected *N. benthamiana* plants showed a photo-bleaching phenotype (Figure 2B). The silencing efficiency was 100.0% in three independent experiments (Supplemental Table S1). We also used TRSV to silence the expression of *eukaryotic initiation factor 4E* (*eIF4E*) and *eukaryotic initiation factor (iso) 4E* [*eIF(iso)4E*] in melon. The results of reverse transcription quantitative polymerase chain reaction (RT-qPCR) showed that the mRNA expression levels of *eIF4E* and *eIF(iso)4E* were significantly decreased (Supplemental Figure S1). Taken together, these results indicated that TRSV can be utilized as an effective VIGS tool in different plants.

TRSV-based silencing of miR166 reduced leaf polarity

To test whether TRSV can be used as a VbMS vector, the well-characterized miR166 was cloned into pTRSV2 using an STTM strategy (Figure 3A; Yan et al., 2012; Sha et al., 2014; Peng et al., 2018; Zhao et al., 2020). By 23 dpi, TRSV2-STTM166-infected *C. melo*, *C. lanatus*, *C. sativus*, and *L. aegyptiaca* plants showed a strong silencing phenotype in which an ectopic leaf outgrew from the vein in the underside of the leaves. The abnormal bilateral symmetric leaves with a double-layered lamina were separated by the midvein due to the alteration of adaxial–abaxial regulation in *C. melo* (Figure 3B). The results of RT-qPCR detection showed that the miR166 level was significantly reduced while the target mRNA level increased in all of the plants infected with TRSV2-STTM166 (Figure 3, C and D). RT-PCR detection confirmed that *STTM166* was expressed in the TRSV-STTM166-infected plants (Figure 3E). The silencing efficiency was 62.5%–87.5% in *C. melo* and *L. aegyptiaca* plants and 12.5%–37.5% in *C. sativus* and *C. lanatus* plants. A similar phenotype was observed in the model plant *N. benhamiana*, in which the silencing efficiency could reach 88.0%–100.0% (Supplemental Figure S2 and Supplemental Table S2). Taken together, these results show that TRSV-based VbMS using the STTM strategy can effectively suppress the miRNA function in cucurbits and *N. benthamiana* plants.

TRSV-based miR159 silencing caused pleiotropic developmental defects in *C. melo* plants

MiR159, which targets *GAMYB* or *GAMYB-like* genes, is one of the most ancient and abundant small RNAs in most land plants (Fahlgren et al., 2007; Jeong et al., 2011; Kozomara et al., 2019; Millar et al., 2019). However, the function of miR159 in cucurbits has remained largely unknown (Liang et al., 2019; Millar et al., 2019). To investigate the miR159-*GAMYB* regulatory circuit in *C. melo*, we modified TRSV to express *STTM159* (Figure 4A). The TRSV-STTM159-infected plants were stunted and the leaves were smaller than the control plants inoculated with TRSV (Figure 4B). Compared with control plants, the miR159 level in TRSV-STTM159-infected plants was significantly decreased while the mRNA level of the target gene *MYB29-like* was significantly increased (Figure 4, C and D). RT-PCR detection demonstrated that the *STTM159* was expressed in *C. melo* plants (Figure 4E). The silencing efficiency was 37.5%–50.0% in *C. melo* plants. A similar phenotype was observed in *N. benthamiana* plants, in which the silencing efficiency was 25.0%–31.3% (Supplemental Figure S3 and Supplemental Table S3). These results indicate that TRSV can effectively block miR159 activity in plants.

TRSV-based VbMS of miR319 caused leaf morphogenesis in *C. lanatus* plants

MiR319, a conserved miRNA family that participates in leaf development, controls the activity of *TEOSINTE BRANCHED1*, *CYCLOIDEA*, and *PROLIFERATING CELL NUCLEAR ANTIGEN BINDING FACTOR (TCP)* genes (Ori et al., 2007; Koyama et al., 2017). To test whether miR319 could suppress the expression of the *TCP4* gene in *C. lanatus*, we modified TRSV to express *STTM319* and inoculated it into watermelon plants (Figure 5A). At 30 dpi, the TRSV-STTM319-infected *C. lanatus* leaves were smaller than the control plants (Figure 5B). The miR319 level was lower and the expression level of the target gene *TCP4* was higher in TRSV-STTM319-infected *C. lanatus* leaves than in the control plants (Figure 5, C and D). RT-PCR detection showed that *STTM319* was expressed in TRSV-STTM319-infected *C.*

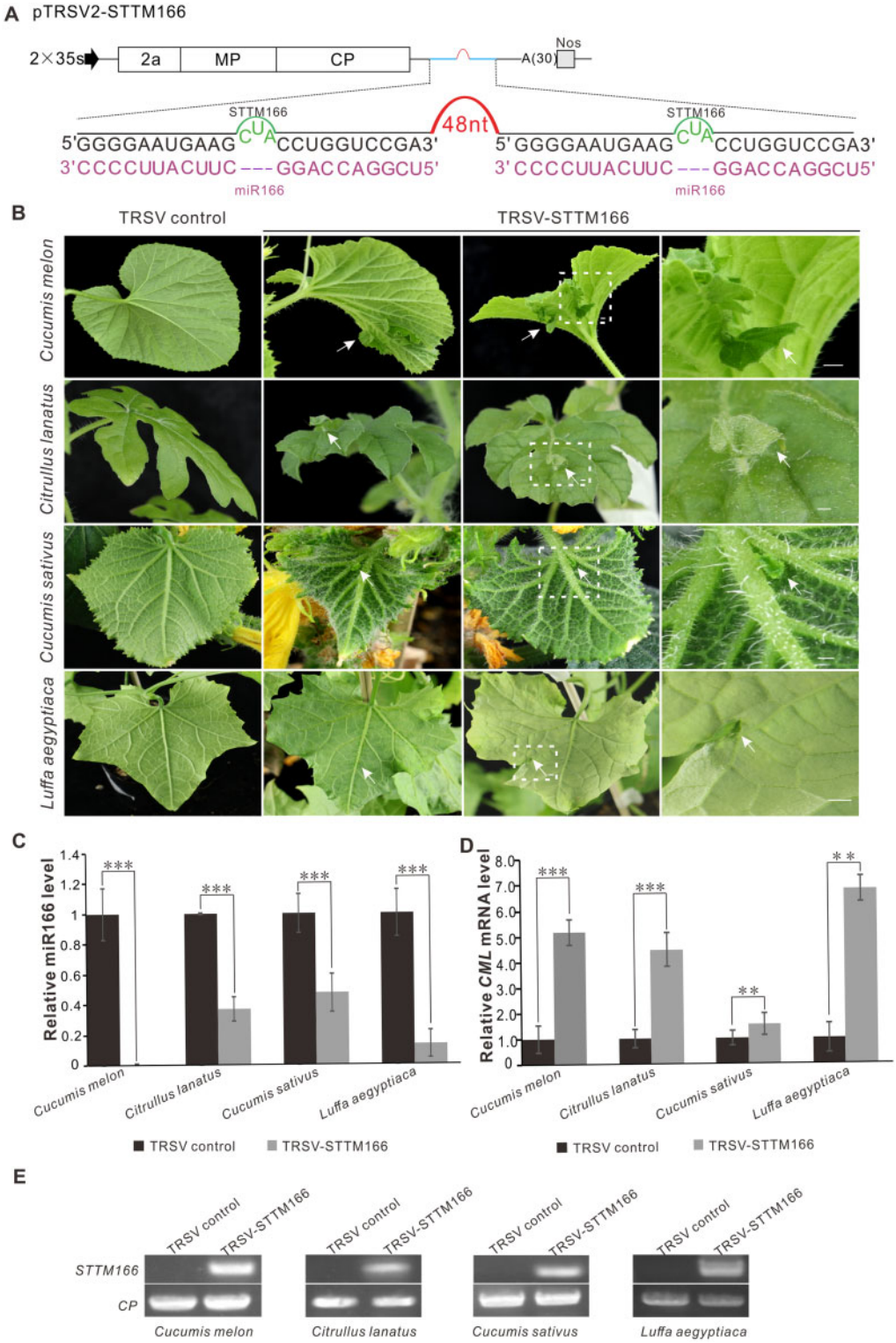

Figure 3 TRSV-based silencing of miR166 in different cucurbits plants. A, Schematic representation of VbMS of mi166. "–-" represents no nucleotide in this position. The STTM166 sequence was introduced into pTRSV2 downstream of the *CP* stop codon. The 48 nucleotides stem-loop spacer contributes to STTM stability and efficiency. B, Leaf phenotypes of plants inoculated with TRSV-STTM166 at 23 dpi. The arrows indicate the ectopic leaf outgrowing from the vein. Scale bars = 1 cm in the third column. The fourth column shows a magnification of dotted rectangle regions in the third column. C, Stem-loop RT-qPCR detection of miR166 level in TRSV- and TRSV-STTM166-infected cucurbits plants. D, Relative expression level of miR166 target gene in various cucurbits plants inoculated with TRSV or TRSV-STTM166. In (C) and (D), the biological experiment was repeated three times. Error bars represent ± SD. Statistical significance between treatments was determined using paired Student's *t* test: $^{*}P < 0.05$, $^{**}P < 0.01$, $^{***}P < 0.001$. E, RT-PCR detection confirmed the TRSV infection as indicated by the presence of *CP* transcripts in all plants and the expression of STTM166

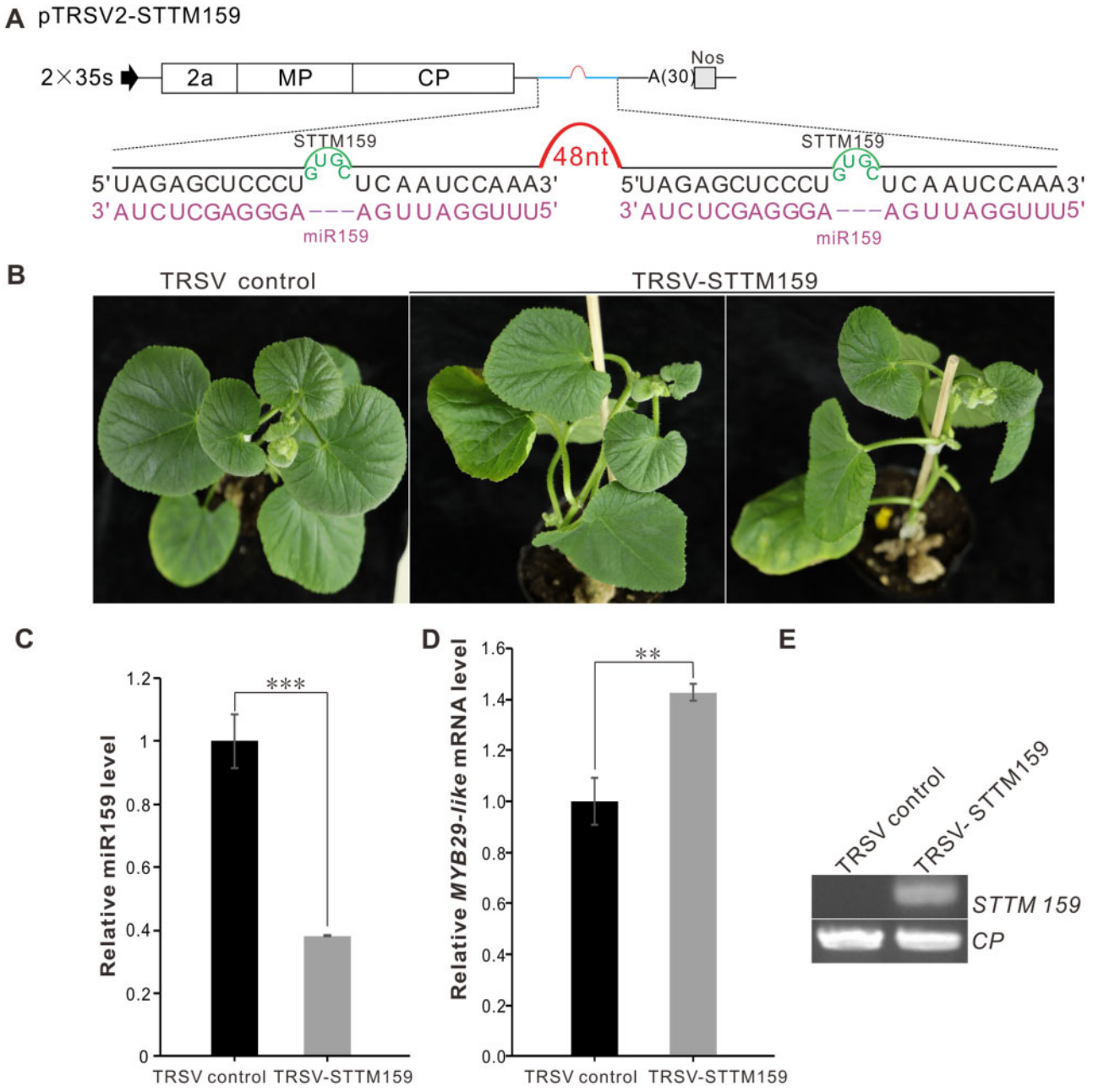

Figure 4 Silencing of miR159 in *C. melo* using TRSV-based VbMS vector. A, Schematic representation of VbMS of miR159. The STTM159 sequence was cloned into pTRSV2 after the *CP* stop codon. "–-" represents no nucleotides in this position. B, Leaf phenotypes of plants inoculated with TSRV and TRSV-STTM159 at 25 dpi. C, Stem-loop RT-qPCR detection of miR159 level in TRSV- and TRSV-STTM159-infected plants. D, Relative expression levels of miR159 target gene *MYBL29-like* in the TRSV- and TRSV-STTM159-infected plants. In (C) and (D), the results were presented as means ± SD from three independent biological replicates. Statistical significance between treatments was determined using paired Student's *t* test: $^{*}P < 0.05$, $^{**}P < 0.01$, $^{***}P < 0.001$. E, RT-PCR detection confirmed the infection of TRSV and the expression of STTM159

lanatus plants (Figure 5E). The silencing efficiency of miR319 was 43.8%–50.0% (Supplemental Table S4). These results indicate that VbMS of miR319 has an impact on leaf development in *C. lanatus* plants.

TRSV-based VbMS of miR172 caused flower development defects in *C. sativus* plants

Arabidopsis miR172 is a crucial regulator of flower organ identity and flower stem cell proliferation (Chen, 2004). Over-expression of a miR172-resistant version of (*APETALA2*) *AP2* elevated AP2 protein levels and led to an indeterminate floral meristem producing supernumerary stamens in Arabidopsis (Zhao et al., 2007). To test whether TRSV-based VbMS of STTM172 could inhibit miR172 activity, we amplified *STTM172* and cloned it into pTRSV2 to generate pTRSV-STTM172 (Figure 6A). Extra petals arose from inner floral meristem in TRSV-STTM172-infected cucumber plants while the control plants grew normally,

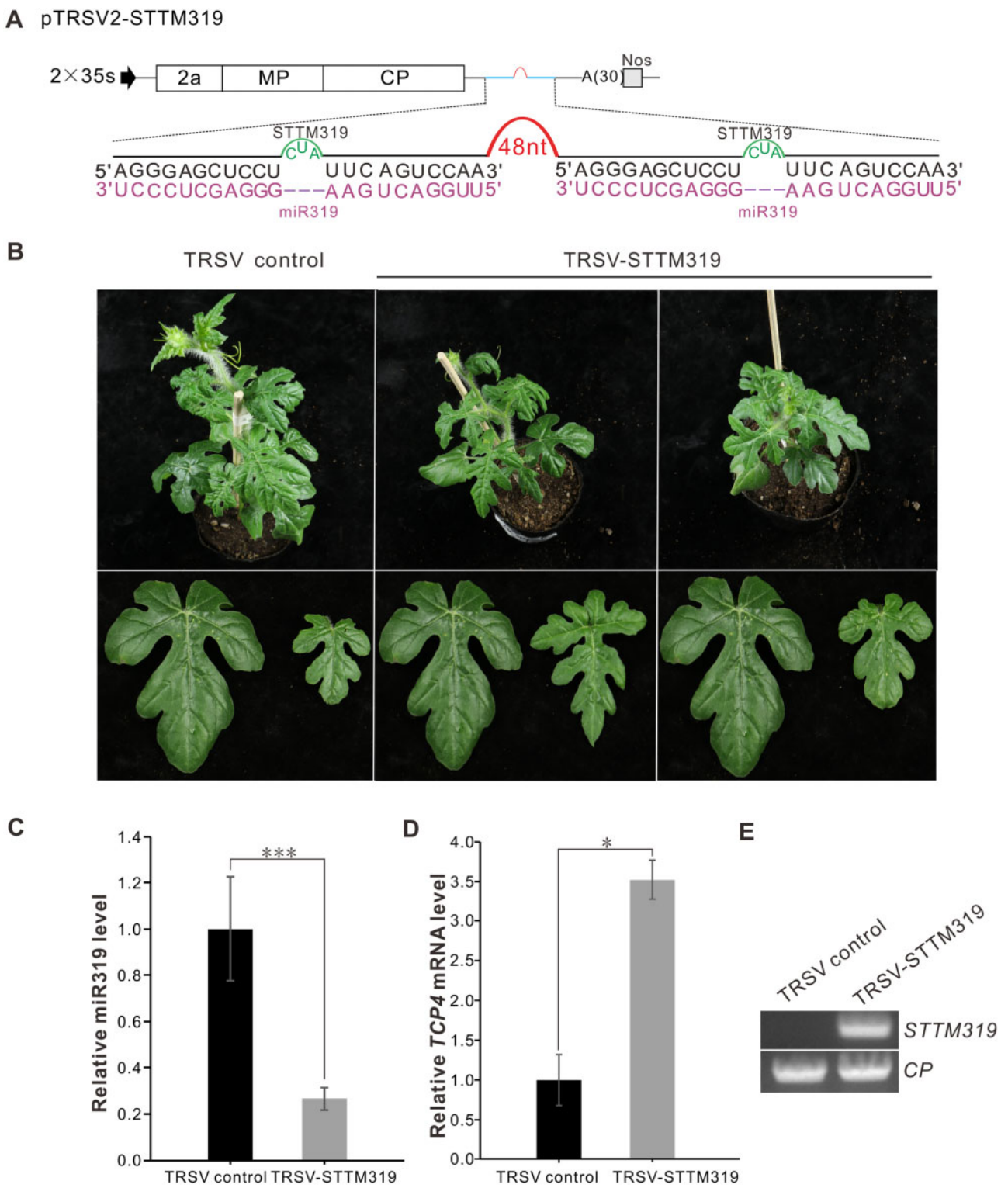

Figure 5 TRSV-based VbMS of miR319 in *C. lanatus*. A, Schematic representation of VbMS of mi319. B, Leaf phenotypes of plants inoculated with TRSV-STTM319 at 30 dpai. C, Stem-loop RT-qPCR analysis of miR319 expression level of TRSV- or TRSV-STTM319-infected plants. D, Detection of the relative expression level of miR319 target gene *TCP4*. In C and D, error bars represent the ± SD of three independent experiments. Statistical significance between treatments was determined using paired Student's *t* test: $^{*}P < 0.05$, $^{**}P < 0.01$, $^{***}P < 0.001$. E, RT-PCR detection confirmed the expression of STTM319 in TRSV-STTM319-infected plants

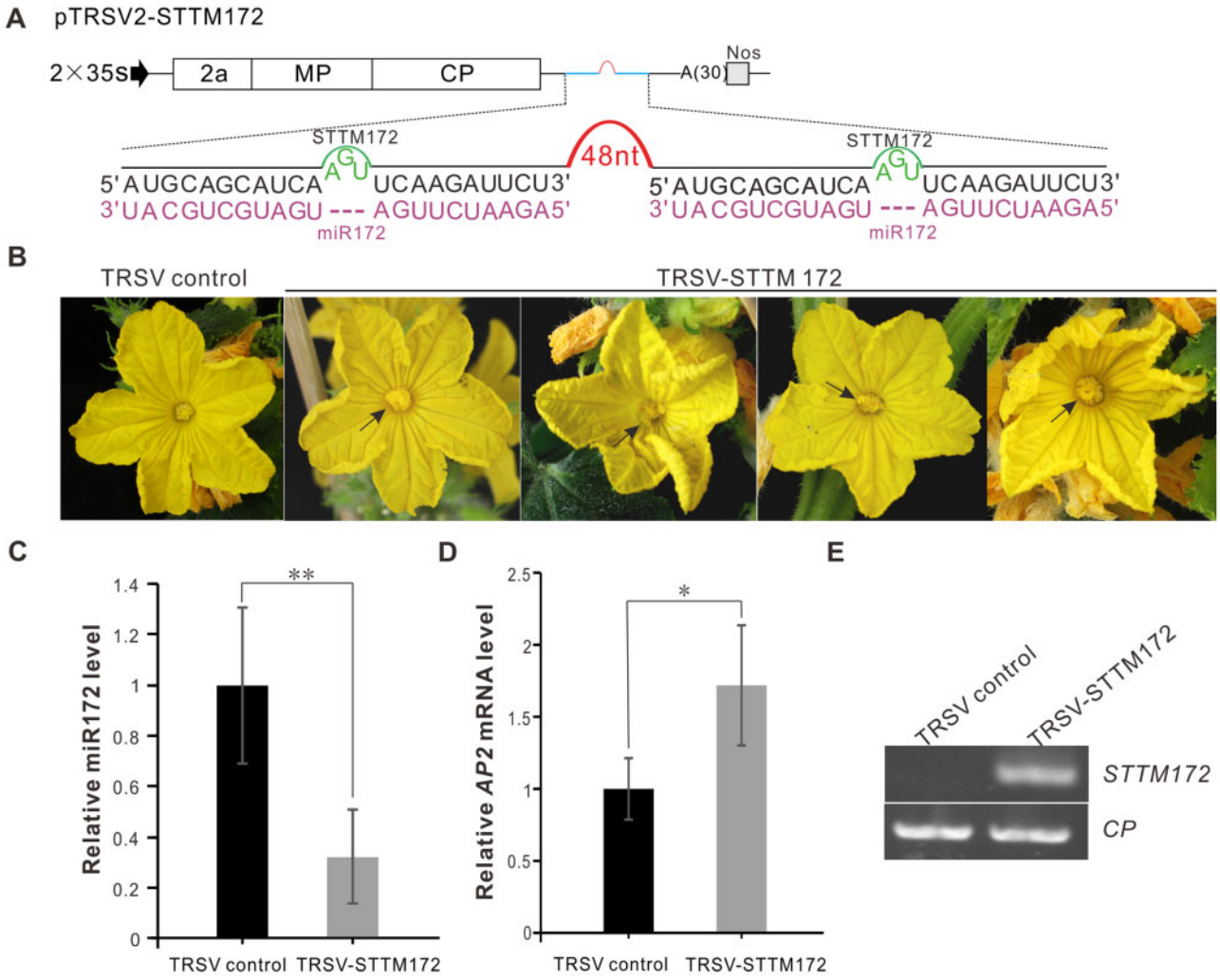

Figure 6 Suppression of miR172 by TRSV-STTM172 in *C. sativus*. A, Schematic representation of TRSV-STTM172. B, The flowers of TRSV- or TRSV-STTM172-infected cucumber plants were photographed at 45 dpi. Arrows indicate the extra petals arising from inner floral meristem. C, Detection of miR172 expression level in TRSV- or TRSV-STTM172-infected plants through stem-loop RT-qPCR. D, The RT-qPCR analysis of relative expression level of miR172 target *RAP2*. In (C) and (D), the results presented were repeated three times. Error bars represent ± SD. Statistical significance between treatments was determined using paired Student's *t* test: $^{*}P < 0.05$, $^{**}P < 0.01$, $^{***}P < 0.001$. E, RT-PCR detection confirmed the expression of miR172 in TRSV-STTM172-infected plants

suggesting that TRSV-based VbMS of miR172 suppressed the function of miR172 (Figure 6B). The miR172 level was lower and the mRNA level of the target gene *C. sativus APETALA2* (*CsAP2*) was higher in TRSV-STTM172-infected cucumber plants than in the control plants (Figure 6, C and D). RT-PCR detection showed that *STTM172* was expressed in TRSV-STTM172-infected cucumber plants (Figure 6E). The silencing efficiency of miR172 in *C. sativus* plants was 25.0%–37.5%. We also inoculated *N. benthamiana* plants with TRSV-STTM172. Flowers in plants inoculated with TRSV-STTM172 displayed shortened petals that could not enclose the interior stamens and carpels. In certain extreme cases, some calyces even turned into petals, causing abnormal flower phenotypes (Supplemental Figure S4B). The level of miR172 in TRSV-STTM172-infected *N. benthamiana* plants was reduced, but the expression level of target gene *NbAP2-LIKE 1 (NbAP2L1)* was increased (Supplemental Figure S4, C and D). The silencing efficiency of miR172 in *N. benthamiana* plants could reach 81.3%–100.0% (Supplemental Table S5). All of these results suggest that TRSV-based VbMS of miR172 using the STTM approach effectively inhibits miR172 function.

Discussion

Some cucurbit species are recalcitrant to genetic transformation. For example, the efficiency in *C. melo* ranges from 0.7% to 7.0% (Fang and Grumet, 1990; Guis et al., 2000; Akasaka-Kennedy et al., 2004; Çürük et al., 2005; Rhimi et al., 2007; Chovelon et al., 2011; Choi et al., 2012; Ren et al., 2012). VIGS provides an alternative strategy to study the function of plant genes. However, very few plant virus-based silencing systems work well in cucurbits (Zhao et al., 2016; Liu et al., 2020). Recently, a cucumber green mottle mosaic virus-based VIGS vector was developed, but it only induced a

silencing phenotype in leaf veins (Liu et al., 2020). TRSV has displayed potential in knocking down the expression of genes in different crop plants (Zhao et al., 2016). Here, we presented a set of TRSV-based vectors with high efficiency in silencing genes or miRNAs in cucurbits, which will help to validate the function of candidate genes involved in agronomic traits. The efficiency of gene silencing was above 80% in *C. melo* and *C. lanatus*, while it was about 35% in *C. sativus* (Supplemental Table S1). This may be due to the infectivity of TRSV in *C. sativus* being weaker than that in *C. melo* and *C. lanatus* plants. In addition to serving as a reverse genetic tool, VIGS is also a forward genetics tool to perform high-throughput genetic screens and functional genomics (Bachan and Dinesh-Kumar, 2012). The TRSV-based VIGS vectors developed in this study can induce a silencing phenotype within 18 d in four important cucurbitaceous plants (Figure 2B). Therefore, they have great potential for rapid and high-throughput forward genetic screens in cucurbits.

Except for engineering TRSV as VIGS vectors, we developed its function in miRNA silencing. This is the first VbMS vector for the function investigation of cucurbit miRNAs. It is noteworthy that the efficiency of most TRSV-based miRNA silencing is high in both model and crop plants. In a previous study, only 20.0%–30.0% of *N. benthamiana* plants expressing target mimics against miR165/166 showed the expected phenotype (Sha et al., 2014). However, all of the TRSV-miR165/166-infected *N. benthamiana* plants showed defective symptoms in leaves (Supplemental Figure S2 and Supplemental Table S2). Furthermore, the silencing efficiency of miRNA was 75.0%–87.6% in *L. aegyptiaca* plants and 68.8%–75.0% in *C. melo*. In most cases, the silencing efficiency of miRNAs in *N. benthamiana* plants was higher than that in cucurbitaceous plants. Only miRNA159 was an exception. In a previous study, no visible phenotype was observed in TRV-miR159-infected *N. benthamiana* plants, but all of the PVX-miR159-infected *N. benthamiana* plants displayed the expected phenotype (Sha et al., 2014; Zhao et al., 2016). Therefore, the development of VbMS systems provides potential solutions for the functional study of some specific miRNAs.

Plant virus-based vectors can be utilized for transient gain-of-function studies, especially in recalcitrant species for genetic transformation (Choi et al., 2019). TRSV can be used to express GFP in *N. benthamiana* plants. However, the GFP fluorescence becomes nearly invisible in newly emerging leaves after 15 dpi (Zhao et al., 2016). The same problem occurred in our study with both *N. benthamiana* and *L. aegyptiaca* plants (Figure 2A). To overcome this drawback, we engineered TRSV into a dual gene expression vector that simultaneously expressed GFP and heterologous VSR separated through two different 2A peptides in tandem. Here, we tested three different VSRs and found that the GFP accumulation in TRSV-GFP-B2-infected plants was slightly higher than that in TRSV-GFP-p19 or TRSV-GFP-2b-infected plants (Figure 1, C and D), which indicated that FHV B2 is more effective for TRSV-based protein expression in *L. aegyptiaca* and *N. benthamiana*. The 2A peptides lead to relatively high levels of downstream protein expression compared with other strategies for multigene co-expression, and they are small in size, thus bearing a lower risk of interfering with the function of co-expressed genes (Donnelly et al., 2001; Liu et al., 2017). Two 2A peptides are different in the sequence, which avoids the loss of foreign genes caused by viral RdRP leap. Different viral 2A peptides are available in the GenBank database and may be used for multiple gene expression of TRSV-based vectors. In addition, we also used TRSV to express *Cas9* from *Staphylococcus aureus* (*SaCas9*, 3,162 bp) in *N. benthamiana* plants (Supplemental Figure S5). The molecular weight of SaCas9 was 124 kDa. The gene-expression capacity of TRSV indicated the possibility of extending the usage of TRSV-based vectors. In recent studies, two plant virus-based vectors were modified for heritable gene editing (Ellison et al., 2020; Ma et al., 2020). It will be interesting to investigate whether TRSV can be used for gene editing in the future.

Taken together, we have shown the great potential of TRSV-based vectors in dissecting the biological roles of genes and miRNA. The versatility of this set of vectors will significantly facilitate functional genomic studies in cucurbitaceous plants.

Materials and methods

Plasmid construction

To construct a full-length infectious clone, the genomic fragments of TRSV RNA1 and RNA2 were obtained by one-step amplification and cloned into the binary vector pCB301 downstream of a double cauliflower mosaic virus (CaMV) 35S promoter to generate pTRSV1 and pTRSV2, respectively. The pTRSV2 vector was further modified to express foreign genes and knockdown endogenous genes or miRNAs.

To improve the foreign gene expression level, the codons for N-terminal 19 amino acids of CP with some nucleotide substitutions for degenerate codons were duplicated and added to the 5′ of the *GFP* and *SaCas9* genes (Zhao et al., 2016). The sequence encoding TaV 2A (5′AGAGCAG AAGGGAGAGGAAGCTTGCTAACCTGTGGAGACGTTGAG GAAAATCCAGGGCCA-3′) was also added to the 3′ of *GFP* and *SaCas9* genes to guarantee the efficient cleavage of GFP. The Arabidopsis (*A. thaliana*) codon-optimized *SaCas9* gene was synthesized as the sequence published previously (Kaya et al., 2016). To construct pTRSV2-GFP-B2, pTRSV2-GFP-P19, and pTRSV-GFP-2b, sequences encoding heterologous VSR and P2A (5′GGCTCGGGCCAGTGTACTAATTATG CTCTCTTGAAATTGGCTGGAGATGTTGAGAGCAACCCAG GTCCC3′) were inserted between the *GFP-T2A* and *CP* region in the pTRSV2-GFP vector through PCR using specific primers as described in Supplemental Table S6.

The *Sna* BI restriction enzyme sequences downstream of the CP translational stop codon were introduced into TRSV RNA2 through one-step site-directed mutation (Liu and

Naismith, 2008). The *CuPDS* gene and *NbPDS* gene were RT-PCR amplified separately from the total RNAs from *C. melo* and *N. benthamiana* leaves using specific primers and inserted into pTRSV2 (Supplemental Table S6). A 48-bp oligonucleotide was utilized as a linker to construct STTM miRNA. The full sequence STTM miRNA was amplified and cloned into pTRSV2 (Yan et al., 2012). All of the constructs were confirmed by DNA sequencing before further use. Primers are listed in Supplemental Table S6.

Plant growth and inoculation

Cucumis melo (cultivar "Huoyingua"), *C. lanatus* (cultivar "Fufengshijilong"), *C. sativus* (cultivar "Nairewangzhongwang"), *L. aegyptiaca* (cultivar "Changfengfiangsigua"), and *N. benthamiana* plants were grown at 22°C in a greenhouse under a 16 h light/8 h dark cycle with 60.0% humidity. Plasmids were individually transformed into *A. tumefaciens* GV3101 cells using a freeze-thaw method (Hofgen and Willmitzer, 1988). The *A. tumefaciens* cultures were grown overnight in Luria–Bertani liquid medium with appropriate antibiotics at 28°C and individually re-suspended in an induction buffer containing 10-mM $MgCl_2$, 10-mM MES, and 150-μM acetosyringone as described earlier (Geng et al., 2015). Separate cultures of *A. tumefaciens* (OD_{600}= 1.0) harboring pTRSV1, pTRSV2, or pBinP19 were mixed in a 1:1:1 ratio and infiltrated into *N. benthamiana* plants. The inoculated plants were grown and observed until the phenotype appeared. The *N. benthamiana* leaves agroinfiltrated with pTRSV2-CuPDS or pTRSV2-miRNA were harvested at 6 dpi for rub-inoculation.

Protein extractions and western blotting

For total protein extraction, plant leaf tissue infected with TRSV was ground in liquid nitrogen followed by suspension in a protein extraction buffer. Samples were boiled for 10 min before centrifugation for 2 min at 10,000*g* at 4°C. The supernatant was kept for SDS-PAGE. Proteins were then transferred into a nitrocellulose membrane in tris-glycine transfer buffer (25-mM Tris base, 192-mM glycine, and 3.5-mM SDS) at 100 V for 60 min. The membrane was then blocked in 5% (w/v) nonfat milk in Tris Buffered Saline with Tween-20 (TBST, 20-mM Tris base, 150-mM NaCl, 0.05% (v/v) Tween-20, pH = 7.5) with gentle agitation for 60 min at room temperature or 4°C overnight. The GFP-specific antibody was added to the nonfat milk at the appropriate dilution. Membranes were washed with TBST three times for 10 min each wash. Secondary goat anti-rabbit IgG conjugated with horseradish peroxidase (Sigma-Aldrich) was incubated for 1 h at a working dilution. The nitrocellulose membranes were then washed briefly with TBS (20-mM Tris base, 150-mM NaCl, pH = 7.5) after two washes in TBST for 10 min each and then photographed. GFP imaging was observed under long-wavelength UV light, and photographs were taken using a Canon 80D camera.

RNA extraction and RT-PCR

Total RNAs were extracted from plant leaves using TransZol reagent (TransGen Biotech, ET101-01). The resulting total RNA samples were treated with a gDNA wiper enzyme (Vazyme, R233-01-AB) to remove plant genomic DNA. Stem-loop RT-PCR was performed to detect the miRNA expression level. Total RNA of 1–5 μg was reverse transcribed using a specific reverse primer and miRNA 1st Strand cDNA Synthesis Kit (Vazyme, MR101-01). Then, PCR was performed using miRNA Universal SYBR qPCR Master Mix (Vazyme, MQ101-01). To detect the target gene level of inoculated plants, 1 μg total RNA (per sample) was reverse transcribed using a HiScriptII Q RT SuperMix kit supplemented with random primers (Vazyme, R222-01-AB). RT-qPCR was conducted using a ChamQ SYBR qPCR Master Mix (Vazyme, Q311-02) on a thermocycler (LightCycler® 96, Roche). The specific detection primers are listed in the Supplemental Table S6. The *CmACTIN* gene was used as an internal control for the detection of miRNA and target genes. The *N. benthamiana eIF4A* and *EF1α* were used as internal controls for the analysis of miRNA and target genes.

Accession numbers

The sequence data of this paper can be obtained from GenBank and the Sol Genomic Network under the following accession numbers: LC376026.1 (CMV *2b*), AJ288942.1 (TBSV *P19*), X77156.1 (FHV *B2*), EU165355.1 (*NbPDS*), XM_011654729 (*CsPDS*), NM_001297480.1 (*CmeIF4E*), XM_008462461.2 [Cm*eIF(ISO)4E*], XM_004137620.3 (*CsCML42*), XM_004137168.3 (*CsTCP4*), XM_031885023.1 (*CsAP2*), Niben101Scf01383g07027.1 (*NbMYBL1*), and CK287095 (*NbAP2L1*).

Supplemental data

The following materials are available in the online version of this article.

Supplemental Figure S1. TRSV-based silencing of *eIF4E* and *eIF(iso)4E* in *C. melo* plants.

Supplemental Figure S2. TRSV-based silencing of miR165/166 in *N. benthamiana* plants.

Supplemental Figure S3. TRSV-based knockdown of miR159 in *N. benthamiana* plants.

Supplemental Figure S4. TRSV-based VbMS of miR172 in *N. benthamiana* plants.

Supplemental Figure S5. The expression of *SaCas9* gene using TRSV in *N. benthamiana* plants.

Supplemental Table S1. Silencing efficiency of *PDS* genes.

Supplemental Table S2. Silencing efficiency of miR166.

Supplemental Table S3. Silencing efficiency of miR159.

Supplemental Table S4. Silencing efficiency of miR319.

Supplemental Table S5. Silencing efficiency of miR172.

Supplemental Table S6. Primers used in this study.

Funding

This study was supported by the National Natural Science Foundation of China (NSFC; 31801704, 31720103912) and the "Taishan Scholar" Construction Project (TS201712023).

Conflict of interest statement. The authors declare no conflict of interest.

References

Abdalla OA, Bruton BD, Fish WW, Ali A (2012) First confirmed report of *Tobacco ringspot virus* in cucurbits crops in Oklahoma. Plant Dis **96:** 1705

Akasaka-Kennedy Y, Tomita KO, Ezura HJPS (2004) Efficient plant regeneration and Agrobacterium-mediated transformation via somatic embryogenesis in melon (*Cucumis melo L.*). Plant Sci **166:** 763–769

Bachan S, Dinesh-Kumar SP (2012) *Tobacco rattle virus* (TRV)-based virus-induced gene silencing. Methods Mol Biol **894:** 83–92

Baltes NJ, Gil-Humanes J, Cermak T, Atkins PA, Voytas DF (2014) DNA replicons for plant genome engineering. Plant Cell **26:** 151–163

Chen X (2004) A microRNA as a translational repressor of *APETALA2* in Arabidopsis flower development. Science **303:** 2022–2025

Choi B, Kwon SJ, Kim MH, Choe S, Kwak HR, Kim MK, Jung C, Seo JK (2019) A plant virus-based vector system for gene function studies in pepper. Plant Physiol **181:** 867–880

Choi JY, Shin JS, Chung YS, Hyung N-I (2012) An efficient selection and regeneration protocol for Agrobacterium-mediated transformation of oriental melon (*Cucumis melo* L. var. *makuwa*). Plant Cell Tiss Organ Cult **110:** 133–140

Chovelon V, Restier V, Giovinazzo N, Dogimont C, Aarrouf J (2011) Histological study of organogenesis in *Cucumis melo* L. after genetic transformation: why is it difficult to obtain transgenic plants? Plant Cell Rep **30:** 2001–2011

Çürük S, Çetiner S, Elman C, Xia X, Wang Y, Yeheskel A, Zilberstein L, Perl-Treves R, Watad AA, Gaba V (2005) Transformation of recalcitrant melon (*Cucumis melo* L.) cultivars is facilitated by wounding with carborundum. Eng Life Sci **5:** 169–177

Ding XS, Mannas SW, Bishop BA, Rao X, Lecoultre M, Kwon S, Nelson RS (2018) An improved *Brome mosaic virus* silencing vector: greater insert stability and more extensive VIGS. Plant Physiol **176:** 496–510

Donnelly MLL, Hughes LE, Luke G, Mendoza H, Dam Et, Gani D, Ryan MD (2001) The 'cleavage' activities of foot-and-mouth disease virus 2A site-directed mutants and naturally occurring '2A-like' sequences. J Gen Mol Virol **82:** 1027–1041

Du Z, Chen A, Chen W, Westwood JH, Baulcombe DC, Carr JP (2014) Using a viral vector to reveal the role of microRNA159 in disease symptom induction by a severe strain of Cucumber mosaic virus. Plant Physiol **164:** 1378–1388

Eamens AL, Agius C, Smith NA, Waterhouse PM, Wang MB (2011) Efficient silencing of endogenous microRNAs using artificial microRNAs in Arabidopsis thaliana. Mol Plant **4:** 157–170

Ellison EE, Nagalakshmi U, Gamo ME, Huang PJ, Dinesh-Kumar S, Voytas DF (2020) Multiplexed heritable gene editing using RNA viruses and mobile single guide RNAs. Nat Plants **6:** 620–624

Fahlgren N, Howell MD, Kasschau KD, Chapman EJ, Sullivan CM, Cumbie JS, Givan SA, Law TF, Grant SR, Dangl JL, et al. (2007) High-throughput sequencing of Arabidopsis microRNAs: evidence for frequent birth and death of *MIRNA* genes. PLoS One **2:** e219

Fang G, Grumet R (1990) *Agrobacterium tumefaciens* mediated transformation and regeneration of muskmelon plants. Plant Cell Rep **9:** 160–164

Franco-Zorrilla JM, Valli A, Todesco M, Mateos I, Puga MI, Rubio-Somoza I, Leyva A, Weigel D, Garcia JA, Paz-Ares J (2007) Target mimicry provides a new mechanism for regulation of microRNA activity. Nat Genet **39:** 1033–1037

Garcia-Mas J, Benjak A, Sanseverino W, Bourgeois M, Mir G, Gonzalez VM, Henaff E, Camara F, Cozzuto L, Lowy E, et al. (2012) The genome of melon (*Cucumis melo* L.). Proc Natl Acad Sci USA **109:** 11872–11877

Geng C, Cong QQ, Li XD, Mou AL, Gao R, Liu JL, Tian YP (2015) DEVELOPMENTALLY REGULATED PLASMA MEMBRANE PROTEIN of *Nicotiana benthamiana* contributes to potyvirus movement and transports to plasmodesmata via the early secretory pathway and the actomyosin system. Plant Physiol **167:** 394–410

Gleba Y, Klimyuk V, Marillonnet S (2007) Viral vectors for the expression of proteins in plants. Curr Opin Biotechnol **18:** 134–141

Gu Z, Huang C, Li F, Zhou X (2014) A versatile system for functional analysis of genes and microRNAs in cotton. Plant Biotechnol J **12:** 638–649

Guis M, Amor MB, Latché A, Pech JC, Roustan JPJSH (2000) A reliable system for the transformation of cantaloupe charentais melon (Cucumis melo L. var. cantalupensis) leading to a majority of diploid regenerants. Sci Hortic **84:** 91–99

Guo S, Zhang J, Sun H, Salse J, Lucas WJ, Zhang H, Zheng Y, Mao L, Ren Y, Wang Z, et al. (2013) The draft genome of watermelon (*Citrullus lanatus*) and resequencing of 20 diverse accessions. Nat Genet **45:** 51–58

Hofgen R, Willmitzer L (1988) Storage of competent cells for *Agrobacterium* transformation. Nucleic Acids Res **16** 9877–9877

Huang S, Li R, Zhang Z, Li L, Gu X, Fan W, Lucas WJ, Wang X, Xie B, Ni P, et al. (2009) The genome of the cucumber, Cucumis sativus L. Nat Genet **41:** 1275–1281

Javier F. Palatnik EA, Wu Xuelin (2003) Control of leaf morphogenesis by micoRNAs. Nature **425:** 257–263

Jeong DH, Park S, Zhai J, Gurazada SG, De Paoli E, Meyers BC, Green PJ (2011) Massive analysis of rice small RNAs: mechanistic implications of regulated microRNAs and variants for differential target RNA cleavage. Plant Cell **23:** 4185–4207

Jian C, Han R, Chi Q, Wang S, Ma M, Liu X, Zhao H (2017) Virus-based microRNA silencing and overexpressing in common wheat (*Triticum aestivum* L.). Front Plant Sci **8:** 500

Jiao J, Wang Y, Selvaraj JN, Xing F, Liu Y (2015) *Barley stripe mosaic virus* (BSMV) induced microRNA silencing in common wheat (*Triticum aestivum* L.). PLoS One **10:** e0126621

Kaya H, Mikami M, Endo A, Endo M, Toki S (2016) Highly specific targeted mutagenesis in plants using *Staphylococcus aureus* Cas9. Scientific Rep **6:** 1–9

Koyama T, Sato F, Ohme-Takagi M (2017) Roles of miR319 and TCP transcription factors in leaf development. Plant Physiol **175:** 874–885

Kozomara A, Birgaoanu M, Griffiths-Jones S (2019) miRBase: from microRNA sequences to function. Nucleic Acids Res **47:** D155–D162

Liang C, Liu H, Hao J, Li J, Luo L (2019) Expression profiling and regulatory network of cucumber microRNAs and their putative target genes in response to cucumber green mottle mosaic virus infection. Arch Virol **164:** 1121–1134

Liao Q, Tu Y, Carr JP, Du Z (2015) An improved cucumber mosaic virus-based vector for efficient decoying of plant microRNAs. Sci Rep **5:** 13178

Liu H, Naismith JH (2008) An efficient one-step site-directed deletion, insertion, single and multiple-site plasmid mutagenesis protocol. BMC Biotechnol **8:** 91

Liu M, Liang Z, Aranda MA, Hong N, Liu L, Kang B, Gu Q (2020) A cucumber green mottle mosaic virus vector for virus-induced gene silencing in cucurbit plants. Plant Methods **16:** 9

Liu Y, Schiff M, Dinesh-Kumar SP (2002) Virus-induced gene silencing in tomato. Plant J **31:** 777–786

Liu Z, Chen O, Wall JBJ, Zheng M, Zhou Y, Wang L, Vaseghi HR, Qian L, Liu J (2017) Systematic comparison of 2A peptides for cloning multi-genes in a polycistronic vector. Sci Rep **7:** 2193

Ma X, Zhang X, Liu H, Li Z (2020) Highly efficient DNA-free plant genome editing using virally delivered CRISPR-Cas9. Nat Plants **6:** 773–779

Millar AA, Lohe A, Wong G (2019) Biology and function of miR159 in plants. Plants (Basel) **8**

Ori N, Cohen AR, Etzioni A, Brand A, Yanai O, Shleizer S, Menda N, Amsellem Z, Efroni I, Pekker I, et al. (2007) Regulation of

LANCEOLATE by miR319 is required for compound-leaf development in tomato. Nat Genet **39:** 787–791

Peng T, Qiao M, Liu H, Teotia S, Zhang Z, Zhao Y, Wang B, Zhao D, Shi L, Zhang C, et al. (2018) A resource for inactivation of microRNAs using short tandem target mimic technology in model and crop plants. Mol Plant **11:** 1400–1417

Ren Y, Bang H, Curtis IS, Gould J, Patil BS, Crosby KMJPCT, Culture O (2012) Agrobacterium-mediated transformation and shoot regeneration in elite breeding lines of western shipper cantaloupe and honeydew melons (*Cucumis melo* L.). Plant Cell Tiss Organ Cult **108:** 147–158

Rhimi A, Hernould M, Boussaid M (2007) *Agrobacterium* mediated transformation of Tunisian *Cucumis melo* cv *maazoun*. Afr J Biotechnol **6**

Robertson D (2004) VIGS vectors for gene silencing: many targets, many tools. Annu Rev Plant Biol **55:** 495–519

Sainsbury F, Canizares MC, Lomonossoff GP (2010) *Cowpea mosaic virus*: the plant virus-based biotechnology workhorse. Annu Rev Phytopathol **48:** 437–455

Senthil-Kumar M, Mysore KS (2014) Tobacco rattle virus-based virus-induced gene silencing in Nicotiana benthamiana. Nat Protoc **9:** 1549–1562

Seo JK, Choi HS, Kim KH (2016) Engineering of soybean mosaic virus as a versatile tool for studying protein-protein interactions in soybean. Sci Rep **6:** 22436

Sha A, Zhao J, Yin K, Tang Y, Wang Y, Wei X, Hong Y, Liu Y (2014) Virus-based microRNA silencing in plants. Plant Physiol **164:** 36–47

Shakiba E, Chen PY, Gergerich R, Li SX, Dombek D, Shi AN, Brye K (2012) Reactions of mid-southern U.S. soybean cultivars to Bean pod mottle virus and Tobacco ringspot virus. Crop Sci **52:** 1980–1989

Shin AY, Koo N, Kim S, Sim YM, Choi D, Kim YM, Kwon SY (2019) Draft genome sequences of two oriental melons, Cucumis melo L. var. makuwa. Sci Data **6:** 220

Vaistij FE, Elias L, George GL, Jones L (2010) Suppression of microRNA accumulation via RNA interference in Arabidopsis thaliana. Plant Mol Biol **73:** 391–397

Wu H, Zhao G, Gong H, Li J, Luo C, He X, Luo S, Zheng X, Liu X, Guo J, Chen J, Luo J (2020) A high-quality sponge gourd (*Luffa cylindrica*) genome. Hortic Res **7:** 128

Wu S, Wang X, Reddy U, Sun H, Bao K, Gao L, Mao L, Patel T, Ortiz C, Abburi VL, et al. (2019) Genome of 'Charleston Gray', the principal American watermelon cultivar, and genetic characterization of 1,365 accessions in the U.S. National Plant Germplasm System watermelon collection. Plant Biotechnol J **17:** 2246–2258

Yan J, Gu Y, Jia X, Kang W, Pan S, Tang X, Chen X, Tang G (2012) Effective small RNA destruction by the expression of a short tandem target mimic in Arabidopsis. Plant Cell **24:** 415–427

Yang J, Zhang TY, Liao QS, He L, Li J, Zhang HM, Chen X, Li J, Yang J, Li JB, Chen JP (2018) Chinese wheat mosaic virus-induced gene silencing in monocots and dicots at low temperature. Front Plant Sci **9:** 1627

Yang L, Mu X, Liu C, Cai J, Shi K, Zhu W, Yang Q (2015) Overexpression of potato miR482e enhanced plant sensitivity to *Verticillium dahliae* infection. J Integr Plant Biol **57:** 1078–1088

Zellner W, Frantz J, Leisner S (2011) Silicon delays Tobacco ringspot virus systemic symptoms in Nicotiana tabacum. J Plant Physiol **168:** 1866–1869

Zhang C, Ghabrial SA (2006) Development of Bean pod mottle virus-based vectors for stable protein expression and sequence-specific virus-induced gene silencing in soybean. Virology **344:** 401–411

Zhang YC, Yu Y, Wang CY, Li ZY, Liu Q, Xu J, Liao JY, Wang XJ, Qu LH, Chen F, et al. (2013) Overexpression of microRNA OsmiR397 improves rice yield by increasing grain size and promoting panicle branching. Nat Biotechnol **31:** 848–852

Zhao F, Hwang US, Lim S, Yoo RH, Igori D, Lee SH, Lim HS, Moon JS (2015) Complete genome sequence and construction of infectious full-length cDNA clones of tobacco ringspot Nepovirus, a viral pathogen causing bud blight in soybean. Virus Genes **51:** 163–166

Zhao F, Lim S, Igori D, Yoo RH, Kwon SY, Moon JS (2016) Development of tobacco ringspot virus-based vectors for foreign gene expression and virus-induced gene silencing in a variety of plants. Virology **492:** 166–178

Zhao J, Liu Q, Hu P, Jia Q, Liu N, Yin K, Cheng Y, Yan F, Chen J, Liu Y (2016) An efficient Potato virus X-based microRNA silencing in *Nicotiana benthamiana*. Sci Rep **6:** 20573

Zhao J, Rios CG, Song J (2020) Potato virus X-based microRNA silencing (VbMS) in Potato. J Vis Exp **159:** e61067

Zhao L, Kim Y, Dinh TT, Chen X (2007) miR172 regulates stem cell fate and defines the inner boundary of APETALA3 and PISTILLATA expression domain in Arabidopsis floral meristems. Plant J **51:** 840–849